



## Parallel ANFIS-GA Lead-Lag Controller for Enhancing Power System Stability with Wind Turbine Integration

Fares ZITOUNI<sup>1,2\*</sup>, Issam GRICHE<sup>1,2</sup>, Mohamed REZKI<sup>1</sup>

<sup>1</sup> Department of Electrical Engineering, Faculty of Applied Sciences, University of Bouira, Bouira 10000, Algeria

<sup>2</sup> Laboratory of Materials, Energy, Water and Environment Processes LPM3E, University of Bouira, Bouira 10000, Algeria

Corresponding Author Email: [f.zitouni@univ-bouira.dz](mailto:f.zitouni@univ-bouira.dz)

Copyright: ©2025 The authors. This article is published by IIETA and is licensed under the CC BY 4.0 license (<http://creativecommons.org/licenses/by/4.0/>).

<https://doi.org/10.18280/jesa.581203>

**Received:** 26 August 2025

**Revised:** 22 October 2025

**Accepted:** 16 December 2025

**Available online:** 31 December 2025

### Keywords:

LL, ANFIS, GA, WT, TCSC

### ABSTRACT

This study explores the stability of power systems, including those with wind farms. A thyristor-controlled series capacitor (TCSC) is utilized to enhance the stability of the power network when wind energy units are integrated. The study presents two novel controllers: the Lead-Lag controller (LL) and the adaptive neuro-fuzzy inference system (ANFIS). Aimed at improving system performance and optimized using Genetic Algorithms (GA). The paper also discusses a hybrid controller for TCSC, termed ANFIS-GA-LL-TCSC, which integrates an ANFIS controller with GA and LL. These controllers were tested on power systems including wind turbines. The GA-LL and ANFIS-GA-LL controllers demonstrated superior performance in enhancing system stability compared to other controllers. Notably, the ANFIS-GA-LL-TCSC controller outperformed others in damping oscillations following disturbances. The study compares the performance of the ANFIS GA LL-TCSC controller with CPSS, ANFIS-CPSS, and GA-LL controllers, highlighting its effectiveness in improving electromechanical eigenvalue positioning and system stability.

### 1. INTRODUCTION

Currently, consumers are meeting their increasing electricity demands by integrating conventional generating units with various renewable energy sources. However, when synchronous generators are taken offline to accommodate increased wind power generation, their ability to reduce oscillation contributions is lost. Consequently, it would be advantageous for wind energy converters to provide damping as an ancillary service [1].

There has been a noticeable change in recent years toward addressing the wide spectrum of production difficulties, transmission, and smart consumption of electrical energy from renewable sources. Wind turbine (WT) electricity generation is particularly valued among alternative energy technologies for meeting global renewable energy targets, due to its cost-free, environmentally friendly, and substantial capacity [2, 3].

Modern wind energy conversion systems primarily employ variable-speed wind turbine generators. In contrast, systems developed prior to the year 2000 were mainly based on fixed-speed induction machines, most commonly the squirrel-cage type (SCIG) [4, 5]. According to research literature, Lead Lag controllers (LL) and power system stabilizers (PSS) have the best coordinated design for wind power integration, which has primarily focused on single-machine systems with less emphasis on multi-machine systems [6, 7]. The literature review shows that optimization techniques are being used more and more to synchronize the integration of the PSS and line commutated converter (LCC), which is very significant.

This tendency has motivated us to propose a new optimization strategy to address this challenge [8]. Modern power transmission systems are often interconnected to efficiently and economically meet growing load demands. These systems, despite facing issues such as transient stability, voltage stability, and small signal stability, are designed to operate close to their operational limits [9]. Small signal stability disturbances typically occur at frequencies between 0.1 and 2.0 Hz, with higher frequency oscillations generally observed in generators located near the load [10, 11]. Low-frequency electromechanical oscillations happen a lot in power systems because their parts are connected to each other. These can be caused by sudden or long-lasting changes in load or the failure of generating or transmission facilities [12, 13].

These rotor oscillations in generators lead to oscillations in other power system variables (bus voltage, transmission line active and reactive power) [14, 15], threatening system security, compromising efficient operation, and impacting small signal stability [16]. PSS are widely applied to mitigate oscillatory behavior in power grids. Nevertheless, their effectiveness can diminish under certain operating conditions, necessitating alternative techniques for effective oscillation damping [17]. Technological advancements in power electronics have given rise to Flexible AC Transmission Systems (FACTS), which significantly contribute to improving power system stability [18, 19]. As defined by IEEE, FACTS devices are systems based on power electronics and static components that regulate key transmission parameters to enhance the controllability and increase the

power transfer capability of AC networks. The implementation of FACTS devices allows for better control of power flows, increased transmission capacity, reduced transmission losses, and enhanced system stability through their fast and flexible operational capabilities [20, 21]. Among these devices, the thyristor-controlled series capacitor (TCSC) has gained prominence, especially for applications involving long transmission lines. TCSCs provide multiple benefits, such as optimizing power flow control, reducing unbalanced components, limiting fault currents, mitigating subsynchronous resonance, damping power oscillations, and improving transient stability [22, 23]. For small-signal stability analyses, the Phillips-Heffron linear model has remained a widely trusted and validated approach over the years. One common stabilization technique involves constructing a stable LL, with parameters determined using optimization methods like particle swarm optimization (PSO) [24-27]. An inappropriate selection of locations and capacities for renewable energy sources (RES) can negatively affect bus voltage profiles, increase active and reactive power losses, and reduce the overall reliability of electrical power systems [28, 29]. Determining the optimal placement and sizing of RES units therefore remains a crucial issue for power system planners and researchers [30-32]. The main objective is to minimize both active and reactive losses while improving steady-state voltage regulation, transient stability, thermal limits of transmission lines, and harmonic performance. However, tuning parameters for the TCSC controller remains complex. While several conventional methods address this tuning challenge, they are iterative, computationally demanding, and converge slowly, making them time-consuming. Lead-Lag blocks have been integrated into complex systems [33] and have proven effective in minimizing errors and rapidly achieving system stability [34, 35]. Therefore, their implementation is introduced in this research using the ANFIS-GA-LL method to enhance the quality of stability solutions. To validate the effectiveness of this controller, various benchmark functions were employed for testing. Additionally, the ANFIS-GA-LL was implemented in a single machine infinite bus (SMIB) system integrated with a wind turbine.

inference system (ANFIS), and an LL for coordinated control. The performance of the proposed solution was compared with traditional controllers, and the results demonstrated a significant enhancement in damping power system oscillations, even with the presence of a wind generator.

Compared to recently reported approaches such as deep reinforcement learning (DRL)-based controllers [35], which require extensive training data and high computational resources, the proposed ANFIS-GA-LL offers a simpler, interpretable structure suitable for real-time implementation. Unlike adaptive PSO techniques that may suffer from premature convergence [36], the GA ensures global exploration of the parameter space. Furthermore, while fuzzy-PID schemes have shown promise, they lack the self-learning capability embedded in ANFIS. Thus, the hybrid parallel design strikes a balance between performance, complexity, and practicality for industrial deployment.

## 2. CASE STUDY DESCRIPTION

The analysis involves an SMIB power system integrated

with a wind turbine. Figure 1 illustrates the case study.

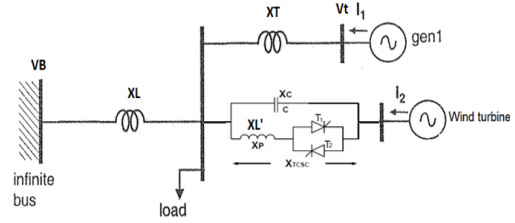


**Figure 1.** Case study

$$\dot{\delta} = \omega_b \Delta \omega \quad (1)$$

$$\dot{\omega} = \frac{1}{M} [P_m - P_e] \quad (2)$$

$$\dot{E}_q = \frac{1}{T_{d0}} \left[ -E_q + E_{fd} \right] \quad (3)$$

$$\dot{E}_{fd} = \frac{K_A}{1+sT_A} [V_R - V_T + V_S] \quad (4)$$

where,

$$P_e = \frac{E_q V_B}{X_{d\Sigma}} \sin \delta - \frac{V_B^2 (X_q - X_d)}{2X_{d\Sigma} X_{q\Sigma}} \quad (5)$$

$$E_q = \frac{X_d \Sigma E_q^{'}}{X_d \Sigma} - \frac{(X_q - X_d^{'})}{X_d \Sigma} V_B \sin 2\delta \quad (6)$$

$$V_{Td} = \frac{X_q V_B}{X_{d\Sigma}} \sin \delta \quad (7)$$

$$V_{Tq} = \frac{X_L E_q^'}{X_{d\Sigma}^'} - \frac{X_d^' V_B}{X_{d\Sigma}^'} \cos \delta \quad (8)$$

$$X_{Eff} = X_T + X_L + X_{TCSC}(\alpha) \quad (9)$$

$$X_{d\Sigma} = X_d + X_L \quad (10)$$

$$X_{q\Sigma} = X_q + X_L \quad (11)$$

$$X_{d\Sigma} = X_d + X_L \quad (12)$$

In stability analysis, several key parameters

In power system stability analysis, several key parameters are defined: the exciter's equivalent electromotive force, represented as  $E_{fd}$ ; the generator's power angle, denoted as  $\delta$ ;  $\omega$  the rotor speed relative to a synchronous reference frame,  $E_q'$ ; the transient voltage along the quadrature axis,  $\omega_b$ ; the system's synchronous speed,  $M$ ; the generator's inertia constant,  $K_A$ ; the gain of the automatic voltage regulator,  $T_A$ ; the regulator's time constant,  $T_{d0}'$ ; the open-circuit time constant along the d-axis,  $V_R$ ; the reference voltage,  $V_S$ ; the supplementary control signal,  $X_d'$ ; the d-axis transient

reactance of the synchronous generator,  $X_q$ ; the q-axis reactance of the synchronous generator,  $V_{Td}$ ; the d-axis terminal voltage,  $X_{TCSC}$ ; and the reactance of the TCSC.

### 3. MODELING OF WIND TURBINES

The mechanical power generated by a wind turbine (WT) is given by the following equation [4]:

$$P_{mw} = \frac{1}{2} \rho_w \cdot A_{rw} \cdot V_w^3 \cdot C_{pw}(\lambda_w, \beta_w) \quad (13)$$

where,  $\rho_w$  represents the air density ( $\text{kg}/\text{m}^3$ ),  $A_{rw}$  refers to the blade swept area ( $\text{m}^2$ ),  $V_w$  indicates the wind speed ( $\text{m}/\text{s}$ ), and  $C_{pw}$  represents the power coefficient of the wind turbine (WT). The power coefficient  $C_{pw}$  is defined by:

$$C_{pw}(\Psi_{kw}, \beta_w) = C_1 \left( \frac{c_2}{\Psi_{kw}} - c_3 \cdot \beta_w - c_4 \cdot \beta_w^{c_5} - c_6 \right) \exp \left( -\frac{c_7}{\Psi_{kw}} \right) \quad (14)$$

$$\frac{1}{\Psi_{kw}} = \frac{1}{\lambda + c_8 \cdot \beta_w} - \frac{c_9}{\beta_w^3 + 1} \quad (15)$$

$$\lambda_w = \frac{R_{bw} \cdot \omega_{bw}}{V_w} \quad (16)$$

In this context,  $\omega_{bw}$  denotes the blade angular speed ( $\text{rad}/\text{s}$ ),  $R_{bw}$  represents the blade radius ( $\text{m}$ ),  $\lambda$  is the tip speed ratio,  $\beta_w$  refers to the blade pitch angle (degrees), and  $c_1$  to  $c_9$  are the constant coefficients used in calculating the power coefficient of the wind turbine. For detailed information on the power coefficients of the wind turbine [15], the wind turbine's cut-in, rated, and cut-out wind speeds are 4 m/s, 15 m/s, and 24 m/s, respectively. When the wind speed is below the rated wind speed ( $V_{w\text{rated}}$ ), the blade pitch angle  $\beta_w$  remains at 0°. Once  $V_w$  exceeds  $V_{w\text{rated}}$ , the pitch-angle control system engages, causing  $(\beta_w)$  to increase.

### 4. DESIGN OF THE PROPOSED CONTROLLERS

#### 4.1 LL

This study employs a LL for the TCSC system. Figure 2 depicts the TCSC with LL.

The washout time constant  $T_W$ , as well as the time constants  $T_2$  and  $T_4$ , are typically predetermined. In this study,  $T_W$  is set to 12 seconds, and  $T_2$  and  $T_4$  are both set to 0.1 seconds. The controller gains  $K_S$ , along with the time constants  $T_1$  and  $T_3$ , will be optimized using the BA algorithm. The equation governing the dynamics of the TCSC reactance is expressed as follows:

$$\Delta X_{TCSC}^{\dot{}} = \frac{1}{T_S} \left( K_S (\Delta X_{TCSC}^{\text{ref}} - \Delta U_{TCSC}) - \Delta X_{TCSC}^{\dot{}} \right) \quad (17)$$

where,  $\Delta X_{TCSC}^{\text{ref}}$  represents the reference reactance of the

TCSC, and  $K_S$  and  $T_S$  denote the gain and time constant of the TCSC, respectively.

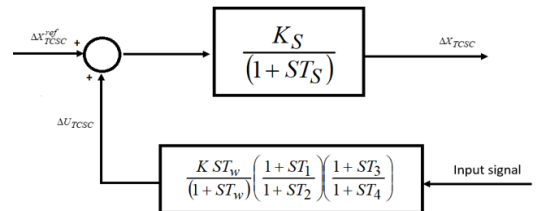


Figure 2. TCSC with LL

#### 4.2 TCSC controller with GA

The GA is a global optimization technique modeled after the principles of natural selection and genetics. In this study, GA is utilized to fine-tune the parameters of the TCSC controller, a crucial process for enhancing power system control performance. Table 1 shows the details of the GA parameters used during the scaling factor adjustment phase.

Table 1. Parameters for GA in tuning stage

Number of Variables	9
Genes Per Variable	3
Chromosome Length	27
Population Size	54
Number of Generations	50

Figure 3 presents the flowchart of the proposed algorithm.

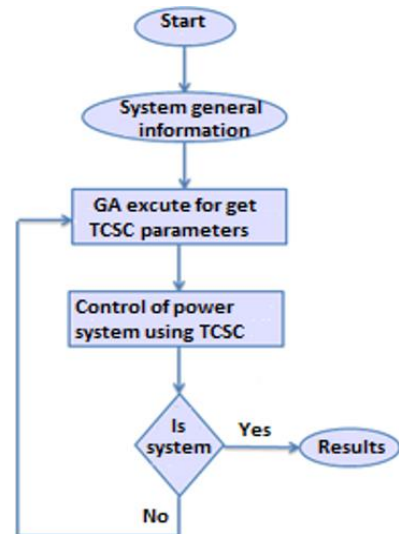


Figure 3. Proposed algorithm flowchart

#### 4.3 Proposed controller

The ANFIS-GA-LL-TCSC controller, Figure 4 illustrates the parallel control system that combines an ANFIS controller with a LL, offering enhanced control performance for the TCSC system.

#### 4.4 Conventional PSS design (PSS)

The PSS incorporates key components, including the stabilizer gain  $K_{PSS}$  a washout block ( $T_W$ ) that functions as a low-pass filter, and phase compensation blocks with time

constants  $T_1$  and  $T_4$ . The rotor speed deviation  $\Delta\omega(syn)$  serves as the input, and the stabilizing signals  $V_{sup}$  and  $V_{sup}$ , limited by an anti-windup device, form the output.

$$V_{sup} = \left[ K_{PSS} \left( \frac{sT_w}{1+sT_w} \right) \left( \frac{1+sT_1}{1+sT_2} \right) \left( \frac{1+sT_3}{1+sT_4} \right) \right] \Delta\omega(syn) \quad (18)$$

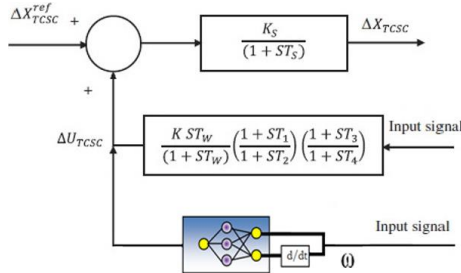


**Figure 4.** Proposed ANFIS-GA-LL-TCSC controller

Figure 5 shows the PSS structure.

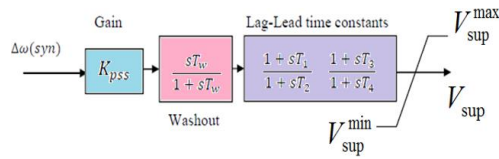


**Figure 5.** PSS structure

#### 4.5 Design of ANFIS proposed

The ANFIS merges the strengths of Neural Networks with those of a fuzzy inference system (FIS) to form a controller aimed at improving the damping of rotor oscillations in synchronous generators by adjusting their excitation. This controller operates based on inputs such as the rotor speed deviation  $\omega$  of the wind generator and the error associated with this deviation. Within the fuzzy logic module, 25 rules are employed to determine the output based on these inputs. The ANFIS controller adapts through a hybrid method that integrates least squares optimization and error backpropagation. Figure 6 depicts the proposed ANFIS controller [4].

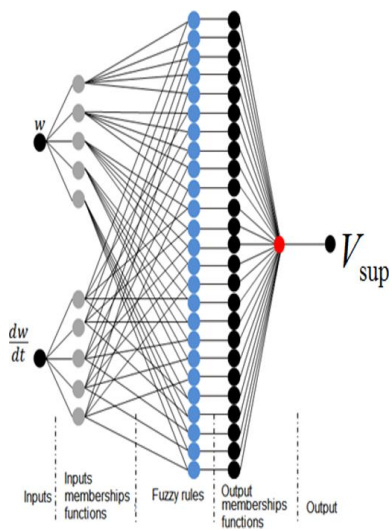


**Figure 6.** Proposed ANFIS controller

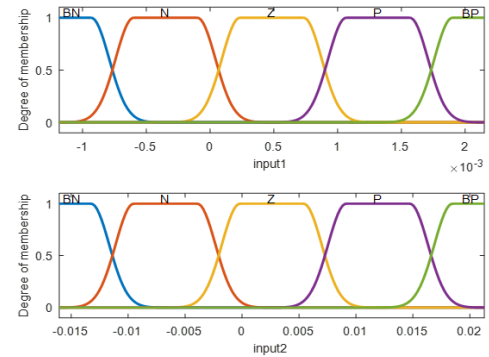


**Figure 7.** Membership function obtained by ANFIS

Figure 7 shows the membership function obtained by ANFIS.

## 5. SIMULATION RESULTS

We evaluated the ANFIS-GA-LL controller's ability to enhance the stability of a power system incorporating a wind turbine during post-disturbance conditions. A comparison with a conventional power system stabilizer (PSS) was conducted to assess its effectiveness. Additionally, the controller's output was determined by calculating the weighted average of the rules.

$$\Delta u_f(k) = \frac{\sum_{i=1}^{25} \omega_i (u_f)_i}{\sum_{i=1}^{25} \omega_i} \quad (19)$$

Table 2 presents the system Eigen values of CPSS and the GA-LL.

**Table 2.** System Eigen values

Without Controller	PSS	With GA-LL
-39.9988	-29.0487	-62.7542
17.4361	$12.3419 \pm j25.5046$	-38.1568
3.5972	$-0.5372 \pm j3.73$	$-0.9574 \pm j30.0752$
-2.8849		$-0.3005 \pm j2.9765$
		-0.1112
		-4.7574

Table 3 shows the optimized parameters of the GA-LL, derived from the Genetic Algorithm (GA) optimization process.

**Table 3.** Optimized parameters using for GA-LL

K	11.0048
$T_1$	0.3921
$T_2$	0.10000
$T_3$	0.5075
$T_4$	10.0999

The proposed method was validated using SMIB system equipped by wind turbine. The system's responses were simulated under varying mechanical power conditions of the

synchronous generator. For the wind turbine, wind speeds between 6 and 12 m/s were classified as sub-synchronous mode, 12 m/s as normal mode, and wind speeds ranging from 12 to 24 m/s as super-synchronous mode. The stability responses of the power system, including the wind turbine with different controllers, are presented in Figures 8 and 9. In these simulations, the conventional LL for the TCSC was replaced with an ANFIS and simulated alongside a Power System Stabilizer (PSS). In the figures, the GA-LL TCSC controller is labeled as GA-LL, and the ANFIS-GA-LL-TCSC controller is labeled as GA-LL. The GA-LL controller outperformed the ANFIS-PSS in reducing overshoot and enhancing stabilization. Furthermore, integrating ANFIS with GA-LL resulted in the ANFIS-GA-LL-TCSC controller exhibiting faster and more efficient responses than GA-LL alone. The figures illustrate that incorporating the ANFIS-GA-LL-TCSC controller leads to a slight decrease in overshoot and a significant improvement in damping for rotor angle and speed compared to systems using GA-LL or ANFIS-CPSS. The design approach of the ANFIS-GA-LL-TCSC controller demonstrates strong performance in stabilizing the system, thereby increasing the power system's stability limit.

The Table 4 shows the quantitative time-domain performance indices provides a more rigorous and comprehensive assessment of the controller's performance.

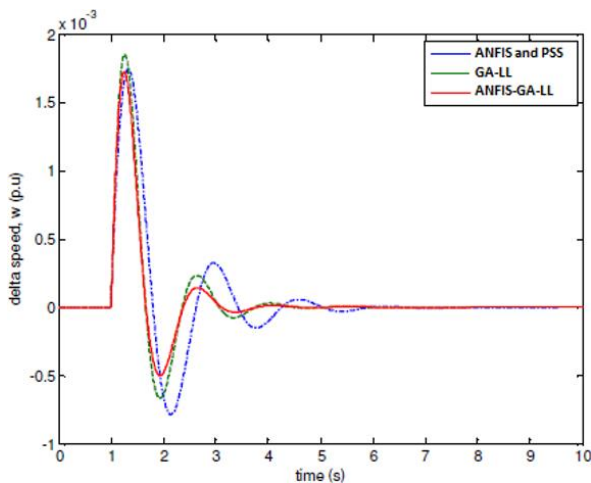


Figure 8. Damping oscillation of speed deviation for SMIB

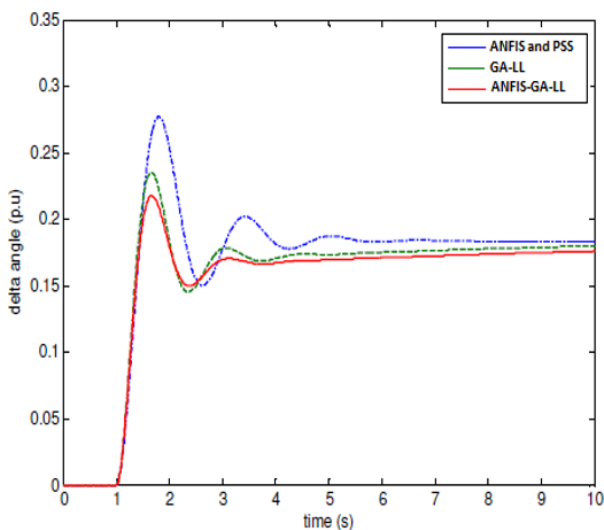


Figure 9. Damping oscillation of speed deviation for SMIB

Table 4. Quantitative time-domain performance

Controller	Overshoot (%)	Settling Time (s)	Stability Margin
PSS	18.2	6.0	moderate
ANFIS-PSS	10.8	4.3	good
GA-LL	8.6	3.4	very good
ANFIS-GA-LL-TCSC	4.2	1.9	excellent

## 6. CONCLUSIONS

This paper proposes a novel hybrid ANFIS-GA-LL-TCSC controller for enhancing small-signal stability in wind-integrated power systems. By combining the adaptive intelligence of ANFIS with the robust phase compensation of a GA-optimized Lead-Lag structure, the parallel controller achieves superior damping performance compared to conventional PSS, ANFIS-PSS, and GA-LL schemes. Simulation results demonstrate faster settling times, reduced overshoot, and improved eigenvalue placement under various operating conditions. The approach offers a practical and effective solution for stabilizing renewable-rich grids. Future work will extend this method to multi-machine systems and hardware-in-the-loop validation.

## REFERENCES

- [1] Cheng, M., Zhu, Y. (2014). The state of the art of wind energy conversion systems and technologies: A review. *Energy Conversion and Management*, 88: 332-347. <https://doi.org/10.1016/j.enconman.2014.08.037>
- [2] Zebar, A., Hamouda, A., Zehar, K. (2015). Impact of the location of fuzzy controlled static var compensator on the power system transient stability improvement in presence of distributed wind generation. *Revue Roumaine des Sciences Techniques, Série Électrotechnique et Énergétique*, 60(4): 426-436.
- [3] Serițan, G., Porumb, R., Cepișcă, C., Grigorescu, S. (2016). Integration of Dispersed power generation. In *electricity distribution: Intelligent solutions for electricity transmission and distribution networks*. Berlin, Heidelberg: Springer Berlin Heidelberg, pp. 27-61. [https://doi.org/10.1007/978-3-662-49434-9\\_2](https://doi.org/10.1007/978-3-662-49434-9_2)
- [4] Griche, I., Messalti, S., Saoudi, K., Touafek, M.Y. (2022). A new adaptive neuro-fuzzy inference system (ANFIS) controller to control the power system equipped by wind turbine. *ITM Web of Conferences*, 42: 01011. <https://doi.org/10.1051/itmconf/20224201011>
- [5] Sava, G.N., Costinas, S., Golovanov, N., Leva, S., Quan, D.M. (2014). Comparison of active crowbar protection schemes for DFIGs wind turbines. In *2014 16th International Conference on Harmonics and Quality of Power (ICHQP)*, Bucharest, Romania, pp. 669-673. <https://doi.org/10.1109/ICHQP.2014.6842860>
- [6] Duong, M.Q., Le, K.H., Grimaccia, F., Leva, S., Mussetta, M., Zich, R.E. (2014). Comparison of power quality in different grid-integrated wind turbines. In *2014 16th International Conference on Harmonics and Quality of Power (ICHQP)*, Bucharest, Romania, pp. 448-452. <https://doi.org/10.1109/ICHQP.2014.6842779>
- [7] Griche, I., Messalti, S., Saoudi, K. (2019). Parallel fuzzy logic and PI controller for transient stability and voltage

regulation of power system including wind turbine. *Przegląd Elektrotechniczny*, 1(9): 53-58. <https://doi.org/10.15199/48.2019.09.10>

[8] Ali, E.S., Abd-Elazim, S.M. (2012). TCSC damping controller design based on bacteria foraging optimization algorithm for a multimachine power system. *International Journal of Electrical Power Energy Systems*, 37(1): 23-30. <https://doi.org/10.1016/j.ijepes.2011.11.001>

[9] Vikal, R., Goyal, G. (2009). TCSC controller design using global optimization for stability analysis of single machine infinite-bus power system. In 2009 15th International Conference on Intelligent System Applications to Power Systems, Curitiba, Brazil, pp. 1-7. <https://doi.org/10.1109/ISAP.2009.5352935>

[10] Kazemi, A., Sohrforouzani, M.V. (2006). Power system damping using fuzzy controlled facts devices. *International Journal of Electrical Power Energy Systems*, 28(5): 349-357. <https://doi.org/10.1016/j.ijepes.2005.09.008>

[11] Griche, I., Messalti, S., Saoudi, K., Touafek, M.Y., Zitouni, F. (2021). A new controller for voltage and stability improvement of multi machine power system tuned by wind turbine. *Mathematical Modelling of Engineering Problems*, 8(1): 81-88. <https://doi.org/10.18280/mmep.080110>

[12] Shojaeian, S., Soltani, J. (2013). Low frequency oscillations damping of power system including unified power flow controller based on adaptive backstepping control. *Revue Roumaine des Sciences Techniques, Série Électrotechnique et Énergétique*, 58(2): 193-204.

[13] Lu, J., Nehrir, M.H., Pierre, D.A. (2004). A fuzzy logic-based adaptive damping controller for static VAR compensator. *Electric Power Systems Research*, 68(2): 113-118. [https://doi.org/10.1016/S0378-7796\(03\)00160-3](https://doi.org/10.1016/S0378-7796(03)00160-3)

[14] Magaji, N., Mustafa, M.W., Bint Muda, Z. (2009). Power system damping using GA based fuzzy controlled SVC device. In TENCON 2009-2009 IEEE Region 10 Conference, Singapore, pp. 1-7. <https://doi.org/10.1109/TENCON.2009.5396011>

[15] Magaji, N., Mustafa, M.W. (2011). Self-learning fuzzy SVC controller for oscillations damping. *Computational Engineering in Systems Applications*, 2: 101-106.

[16] Yuan, Z., De Haan, S.W., Ferreira, J.B., Cvoric, D. (2010). A FACTS device: Distributed power-flow controller (DPFC). *IEEE Transactions on Power Electronics*, 25(10): 2564-2572. <https://doi.org/10.1109/TPEL.2010.2050494>

[17] Shahgholian, G., Movahedi, A. (2014). Coordinated design of thyristor-controlled series capacitor and power system stabilizer controllers using velocity update relaxation particle swarm optimization for two-machine power system stability. *Revue Roumaine des Sciences Techniques*, 59(3): 291-301.

[18] Panda, S., Padhy, N.P. (2007). Coordinated design of TCSC controller and PSS employing particle swarm optimization technique. *International Journal of Computer and Information Engineering*, 1(5): 269-277.

[19] Griche, I., Messalti, S., Saoudi, K. (2021). Instantaneous power control strategy for voltage improvement in power network equipped by wind generator. *Journal Européen des Systèmes Automatisés*, 54(1): 147-154. <https://doi.org/10.18280/jesa.540117>

[20] Jalilzadeh, S., Noroozian, R., Tirtashi, M.R.S., Farhang, P. (2011). Comparison of TCSC and PSS state feedback controller performances on damping of power system oscillations using PSO. In 2011 19th Iranian Conference on Electrical Engineering, Tehran, Iran, pp. 1-5.

[21] Padiyar, K.R. (1996). *Power System Dynamics: Stability and Control*. (Wiley).

[22] Pham, D.T., Ghanbarzadeh, A., Koç, E., Otri, S., Rahim, S., Zaidi, M. (2006). The bees algorithm-a novel tool for complex optimisation problems. In *Intelligent Production Machines and Systems*, pp. 454-459. <https://doi.org/10.1016/B978-008045157-2/50081-X>

[23] Gu, Q., Pandey, A., Starrett, S.K. (2003). Fuzzy logic control schemes for static VAR compensator to control system damping using global signal. *Electric Power Systems Research*, 67(2): 115-122. [https://doi.org/10.1016/S0378-7796\(03\)00077-4](https://doi.org/10.1016/S0378-7796(03)00077-4)

[24] Kundur, P. (2007). Power system stability. *Power System Stability and Control*, 10(1): 7-1.

[25] Fang, D.Z., Xiaodong, Y., Chung, T.S., Wong, K.P. (2004). Adaptive fuzzy-logic SVC damping controller using strategy of oscillation energy descent. *IEEE Transactions on Power Systems*, 19(3): 1414-1421. <https://doi.org/10.1109/TPWRS.2004.831686>

[26] Engelbrecht, A.P. (2007). *Computational Intelligence: An Introduction* (Vol. 2). Hoboken, NJ, USA: John Wiley Sons. <https://doi.org/10.1002/9780470512517>

[27] Abd mouleh, Z., Gastli, A., Ben-Brahim, L., Haouari, M., Al-Emadi, N.A. (2017). Review of optimization techniques applied for the integration of distributed generation from renewable energy sources. *Renewable Energy*, 113: 266-280. <https://doi.org/10.1016/j.renene.2017.05.087>

[28] Viral, R., Khatod, D.K. (2012). Optimal planning of distributed generation systems in distribution system: A review. *Renewable and Sustainable Energy Reviews*, 16(7): 5146-5165. <https://doi.org/10.1016/j.rser.2012.05.020>

[29] Kola, S.S. (2018). A review on optimal allocation and sizing techniques for DG in distribution systems. *International Journal of Renewable Energy Research*, 8(3): 1236-1256. <https://doi.org/10.20508/ijrer.v8i3.7344.g7424>

[30] Pan, W.T. (2012). A new fruit fly optimization algorithm: Taking the financial distress model as an example. *Knowledge-Based Systems*, 26: 69-74. <https://doi.org/10.1016/j.knosys.2011.07.001>

[31] David, B.F. (1998). Artificial Intelligence through Simulated Evolution. In *Evolutionary Computation: The Fossil Record*, pp. 227-296. <https://doi.org/10.1109/9780470544600.ch7>

[32] Simon, D. (2008). Biogeography-based optimization. *IEEE Transactions on Evolutionary Computation*, 12(6): 702-713. <https://doi.org/10.1109/TEVC.2008.919004>

[33] Babesse, S. (2019). Design of two optimized controllers of a hydraulic actuator semi-active suspension. *Engineering, Technology Applied Science Research*, 9(4): 4561-4565. <https://doi.org/10.48084/etasr.2836>

[34] Gong, Y., Kim, I., Choi, W. (2025). Improved control of multi terminal direct current voltage source converters using proportional integral and lead lag controllers. *Scientific Reports*, 15(1): 5368. <https://doi.org/10.1038/s41598-025-89205-8>

[35] Shahgholian, G., Fattollahi, A. (2017). Improving power

system stability using transfer function: A comparative analysis. *Engineering, Technology Applied Science Research*, 7(5): 1946-1952.  
<https://doi.org/10.48084/etasr.1341>  
[36] Bera, P.K., Kumar, V., Pani, S.R., Malik, O.P. (2023).

Autoregressive coefficients based intelligent protection of transmission lines connected to type-3 wind farms. *IEEE Transactions on Power Delivery*, 39(1): 71-82.  
<https://doi.org/10.1109/TPWRD.2023.3321844>